International Journal of Chemical, Materials and Biomolecular Sciences
ISSN: 2415-6620
Vol:9, No:12, 2015

Construction of Strain Distribution Profiles of EDD Steel at Elevated Temperatures

Eshwara K. Prasad, Raman R. Goud, Swadesh Kumar Singh, N. Sateesh

***Abstract*—**In the present work, forming limit diagrams and strain distribution profile diagrams for extra deep drawing steel at room and elevated temperatures have been determined experimentally by conducting stretch forming experiments by using designed and fabricated warm stretchforming tooling setup. With the help of forming Limit Diagrams (FLDs) and strain, distribution profile diagrams the formability of Extra Deep Drawing steel has been analyzed and co-related with mechanical properties like strain hardening COEFFICIENT (n) and normal anisotropy ($\bar{r}$). Mechanical properties of EDD steel from room temperature to 450^0C were determined and discussed the impact of temperature on the properties like work hardening exponent (n) anisotropy (r-) and strength coefficient of the material. In addition, the fractured surfaces after stretching have undergone the some metallurgical investigations and attempt has been made to co-relate with the formability of EDD steel sheets. They are co-related and good agreement with FLDs at various temperatures.

***Keywords*—**FLD, microhardness, strain distribution profile, stretch forming.

I. Introduction

SHEET metal is a critical material for vehicle design, due to its design versatility and manufacturability. Low carbon sheet steel has long been the workhorse material in consumer industries because it can be stamped into inexpensive, complex components at very high production rates. There has been a continuing trend towards development of materials with improved formability, which led to development of extra deep drawing quality (EDDQ) steel sheets.

According to literature various factors like, tool geometry, friction [1], and strain path changes [2], [3] strain rate sensitivity, grain size [5], [6], [8] anisotropy, strainhardening exponent [9], [10] , influences the formability of the material and hence on the formability limit diagrams. The formability of steel sheets can also depend on sheet thickness [12], [13], [15] that increase in limit strains with increase in sheet thickness. They suggested that this trend is associated with the ability to resist the localized necking as thickness increase. It was also shown that significant improvement in FLD level due to increase in sheet thickness could be obtained, particularly in the biaxial stretching region. Some investigations on ferrous alloys like Aluminum (Al) alloys [18]-[20] low carbon steels [11], [12], [14], [17] have done remarkable work on forming limit diagrams and impact of mechanical properties on formability of the materials.

In the present work, EDD steel material sheets were cut into square and rectangular blanks of size 110X110mm to 110X20mmand stretched on specially designed die punch assembly by using hydraulic press. The experimentation was carried out in three different regions namely safe, necking and fractured. The strains were measured and FLDs were plotted by taking major strain as ordinate and minor strain as abscissa. In addition, the strain distribution profiles, which represent train distribution in the material during stretchforming under different states, were plotted. Later on fractured surfaces are mounted and under gone the fractography.

II. Experimental Procedure

A. Chemical Composition &Tensile Test

The chemical composition of EDD steel sheets used in the experiments was found out by spectrometry and the same is presented in Table I. Tensile tests were carried out by using electronic universal testing machine of 5 tonne capacity. The samples were prepared by cutting the EDD sheets along three different directions namely 0◦, 45◦ and 90◦ to the rolling direction of the sheets.

TABLE I
CHEMICAL COMPOSITION OF *EDD* STEEL

Element	% of weight
Carbon	0.048
Silicon	0.83
Manganese	0.39
Sulphur	0.024
Phosphorus	0.019
Chromium	0.027
Stannum	0.004
Copper	0.019
Nickel	0.054
Molybdenum	0.028
Ferrous	Rest

The load versus extension data were obtained from these test. The strain hardening exponent (n), the plastic strain ratio (r) (which is the ratio of the width strain to the thickness strain) and planer anisotropy ($\bar{r}$) which are important factors that indicate the formability of the sheet metals were determined from the tensile tests. Using the equation $\sigma = K\varepsilon^n$, where σ is true stress and ε is true strain, K strength coefficient was found out. $\bar{r}$ values along three directions namely parallel (0^0), diagonal (45^0) and perpendicular (90^0) to the rolling

Eswar Prasad K. is with the Jawaharlal Nehru Technological University, Hyderabad, India (Corresponding author, phone: +919701702015; e-mail: epkoorapati@gmail.com).
Swadesh Kumar Singh, Sateesh N. and Raman Goud R. are with the Mechanical Engineering Department, GRIET affiliated to JNT University, Hyderabad, India (e-mail: Swadesh@griet.ac.in, nagarisateesh007@gmail.com, ramangoud@griet.ac.in).

direction were found out using tensile test. The normal anisotropy$\bar{r}$and the planer anisotropy (Δr) were calculated from the $\bar{r}$ values determined along three directions namely parallel (0^0), diagonal (45^0) and perpendicular (90^0) to the rolling direction using the following expressions:

$$\bar{r} = (r_0 + r_{90} + 2r_{45})/4 \quad (1)$$

$$\Delta r = (r_0 + r_{90} - 2r_{45})/2 \quad (2)$$

B. Stretchforming Test & Forming Limit Diagrams

The forming limit diagrams were evaluated by following Hecker's simplified technique [4]. In this method, mainly the experimental procedure involves three stages namely1) Grid marking on the specimen sheets, 2) Stretching the grid-marked samples to failure or onset of localized necking or safe and finally 3) Measurement of strains.

Fig. 1 Stretchforming experimentation test rig

Grid marking on the EDD steel sheets specimens was done by etching process using a non-contacting grid of 5 mm diameter circle pattern. The grid pattern was etched on the specimens using an electro-chemical etching machine. Placing the grid marked specimen on the lower die of punch die assembly setup and stretching experiments were carried out on a 20 tonne (20t) capacity hydraulic press shown in Fig. 1. The punch-die assembly was designed and fabricated depending on the thickness of the sheets. A typical punch-die assembly used in the experiments is shown in Fig. 2 The sheet samples were subjected to different states of stain, i.e. the tension-tension zone, plane strain and the tension-compression zone by varying the width of the sample. In this method, samples were cut using sharing machine. The length of the blank was 110 mm and width was varied between 110 to 20 mm insteps of 10 mm. For each blank width, at least five specimens were tested for each temperature to get maximum number of data points. To obtain the maximum values in the magnitude of the negative minor strain, uniaxial tension tests were also done using grid-marked of localized specimens. The blanks were stretched to before necking i.e. safe, the experiments were stopped at the time of onset of localized necking in some cases and continued until fracture in other cases. The circles on the sheet samples became ellipses after stretching, falling into safe, necked, and failed zones. The major and minor diameters of the ellipses were measured using a travelling microscope with an accuracy of 0.01mm.Major strains and minor strains were calculated in three regions. FLD was drawn by plotting the minor strain in abscissa and corresponding major strain in ordinate and by drawing a curve, which separates the safe region from the unsafe region. The forming limit curves were drawn by connecting the necking strains for various blanks of an EDD steel sheets. The accuracy of the FLD lies well within a band of ±2% in the engineering strain values.

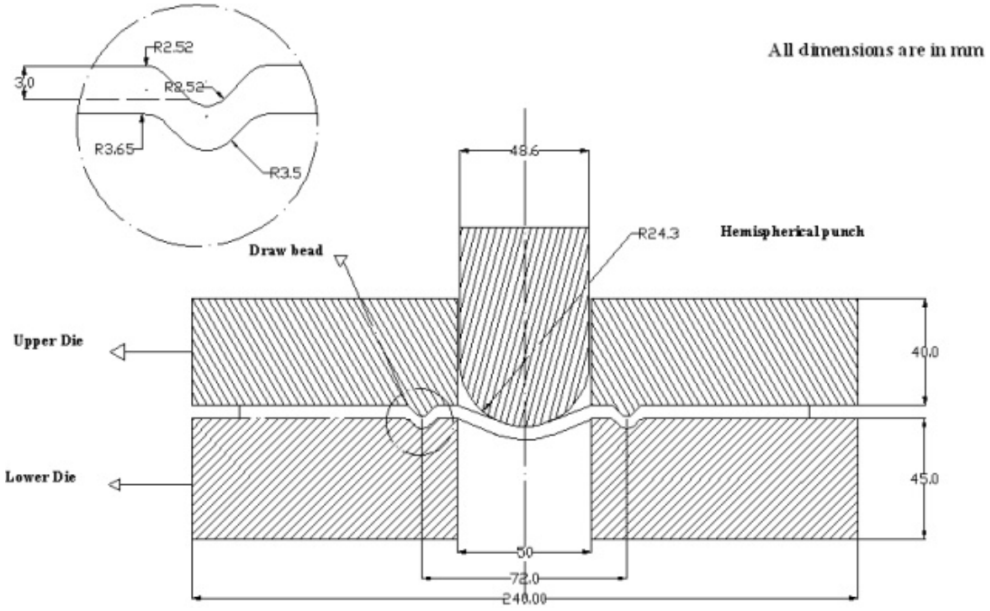

Fig. 2 Punch –Die assembly

C. Strain Distribution Profile

The strain distribution in the material during stretchforming under different states of strain, were best represented by strain distribution profiles. The specimens of different blank width, which were deformed under stretchforming onto the onset of severe localized necking or fracture were selected. The major strains and minor strains were measured for all the ellipses along the longitudinal direction and distance from the pole of the each specimen, which represent the radial and tangential strains in the samples at those locations. The ellipse, which lies exactly under the punch usually, undergoes minimum deformation and it lies at the center of the longitudinal meridian of the deformed specimen. The center of this ellipse is referred to as the pole. The radial and tangential strains were plotted as a function of their distance from the pole, which termed as strain distribution profiles.

D. Metallurgical Studies

Samples for optical microscopy prepared by standard metallography practice were observed under the optical microscope with a view to obtaining microstructural aspects. Specimens were polished and etched using a nitric acid-amyl alcohol [16]. The average grain sizes of the all EDD steel sheet in the as-received condition were determined by the linear intercept method.

The fractured surfaces of the specimens (with three different blank widths deformed to failure under different modes) were examined using a 200X microscope. The fractured samples were carefully preserved after the punch-stretching experiments. Specimens for fractography examination were cut from regions closest to the origin of cracks. These samples were cleaned and etched with nital (2%) before examining under the microscope. The main features of the fracture were analyzed and an attempt has been made to correlate with formability.

III. Results and Discussion

A. Chemical Composition and Tensile Properties

The tensile parameters namely strain hardening exponent (n) and strength coefficient (K) of various steel sheets taken for study obtained from the tensile tests are tabulated in Table II.

TABLE II
MECHANICAL PROPERTIES

Temp	25^{0}C	150^{0}C	300^{0}C	450^{0}C
UTS	337	304	294	329
YS	202	188	184	216
Strain at YS	0.0222	0.0291	0,0314	0,0582
elongation	44	35	29	39
K	677	577	548	684
n	0.304	0.274	0.261	0.289

UTS = Ultimate Tensile Strength, YS =Yield strength, K = Strength coefficient; n= Work hardening exponent, Temp = Temperature.

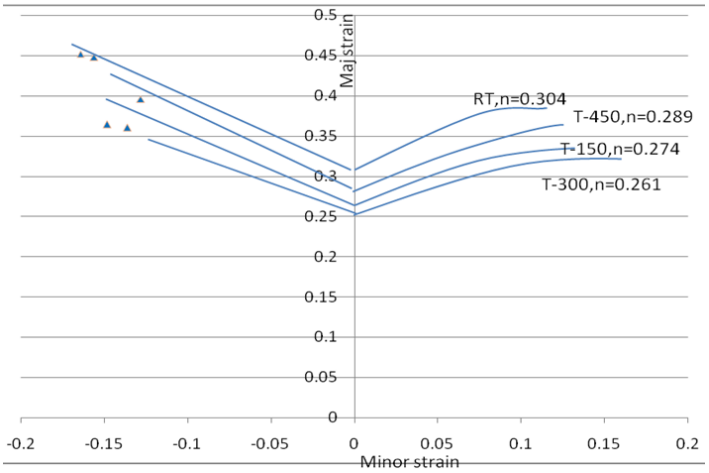

Fig. 3 Combined formability limit diagrams

B. Forming Limit Diagrams

The forming limit and fracture limit diagrams for different temperatures are shown in Fig. 3. The strain combinations above the FLD line will lead to fracture and those below the line will produce safe region in the drawn cup.

FLDs were determined experimentally for the EDD steel sheets by following Hecker's simplified technique [4] are shown in Fig. 3. The above FLDs have shown that stretchability of sheet metal is strongly influenced by the value of strain hardening exponent (n).The n values of EDD steel sheets are shown in Table II. From the table it can be seen that the values obtained from true uniform strain in tensile test agreed well with the FLDs obtained at room temperature, 150^{0}C, 300^{0}C, and 450^{0}C mainly in plain strain region. The formability of EDD steel at room temperature, 150^{0}C, 300^{0}C and 450^{0}C temperatures are consistent with expectations based on the uniaxial tensile properties. The effect of temperature on EDD steel sheets is observed the level of the FLD is clearly seen, particularly at the plain strain conditions. The level of the FLD decreased with increase in sheet temperature, which is approximately coincident with strain hardening exponent (n) at each considered temperature. However, the level of FLD

was increased at temperature of 450^{0}C irrespective of increase in temperature. It is because by increasing the temperature further there was effect of sensitivity index and also dynamic strain regime starts appearing in the material near this temperature [7], [8]. It can be seen the Table II that at 450^{0}C there is increase in strength, strength coefficient and relative increase in the work hardening.

It can be seen from the FLDs that as the temperature increases, strain data points in the neck and also in the fracture region, there is a downward trend in these data points towards biaxial stress line. It is primarily because as the temperature increases, there will be decrease in the mean flow stresses and lesser amount of load will be required to deform the material. This phenomenon can be seen in the load- displacement graphs that by increasing the temperature of specimen, there is decrease in the load requirement in all the samples. There is slight increase in the load at 4500C as compared to 3000C because of dynamic strain regime where there is an increase in work hardening coefficient and as a result of that strain data points in the biaxial stress region is having slight upward trend. It can be seen from load-displacement graphs that by decreasing the width of strip, similar trend in the data was observed.

B. Strain Distribution Profiles

The strain distribution profile were determined at room temperature, 150^{0}C, 300^{0}C, and 450^{0}C and shown in Figs. 4-8. The following observations were found from the strain distribution profiles:

1. From the measured strain distributions in the stretched specimens, two distinct peaks were observed in major strain for all the blank width and these peaks were located symmetrically on either side of the pole. The asymmetry observed in the magnitude of strain peaks on either side of the pole could be due to the fact that when fracture initiated on one side of the pole, the load ceased to act on the other side which was in either safe or necked zone and hence the deformation did not proceed further in that region.

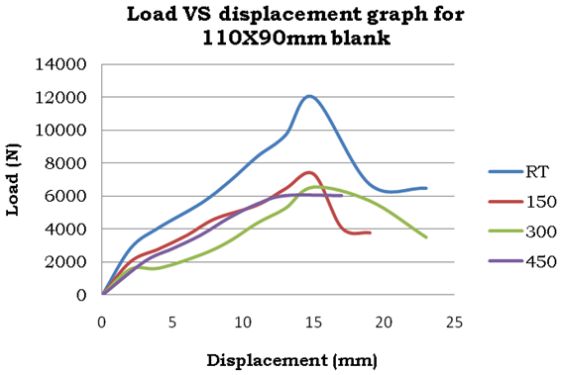

Fig. 4 Load vs Displacement graph

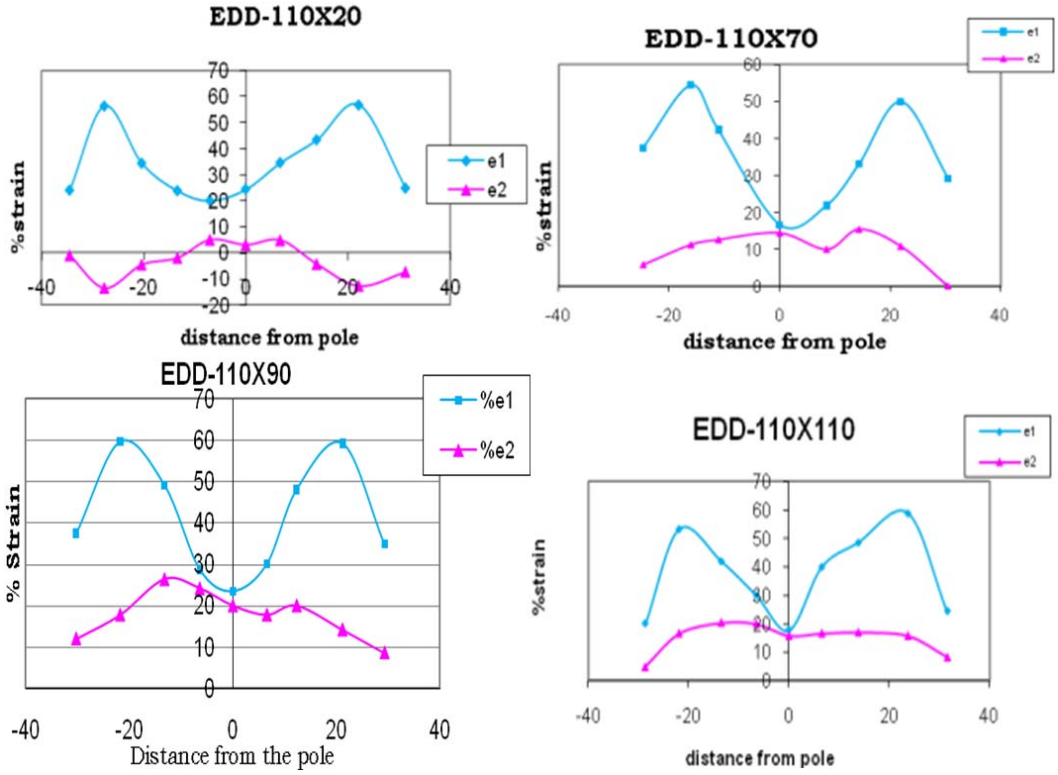

Fig. 5 Strain Distribution Profiles at room temperature

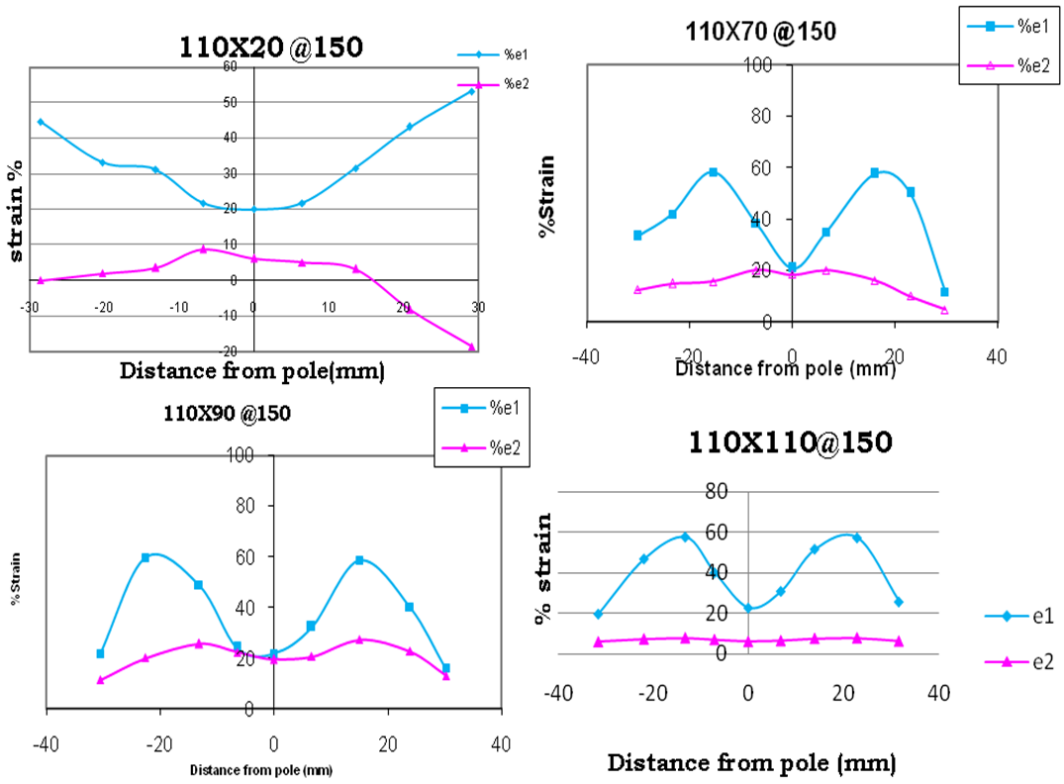

Fig. 6 Strain Distribution Profiles at 150^{0}C temperature

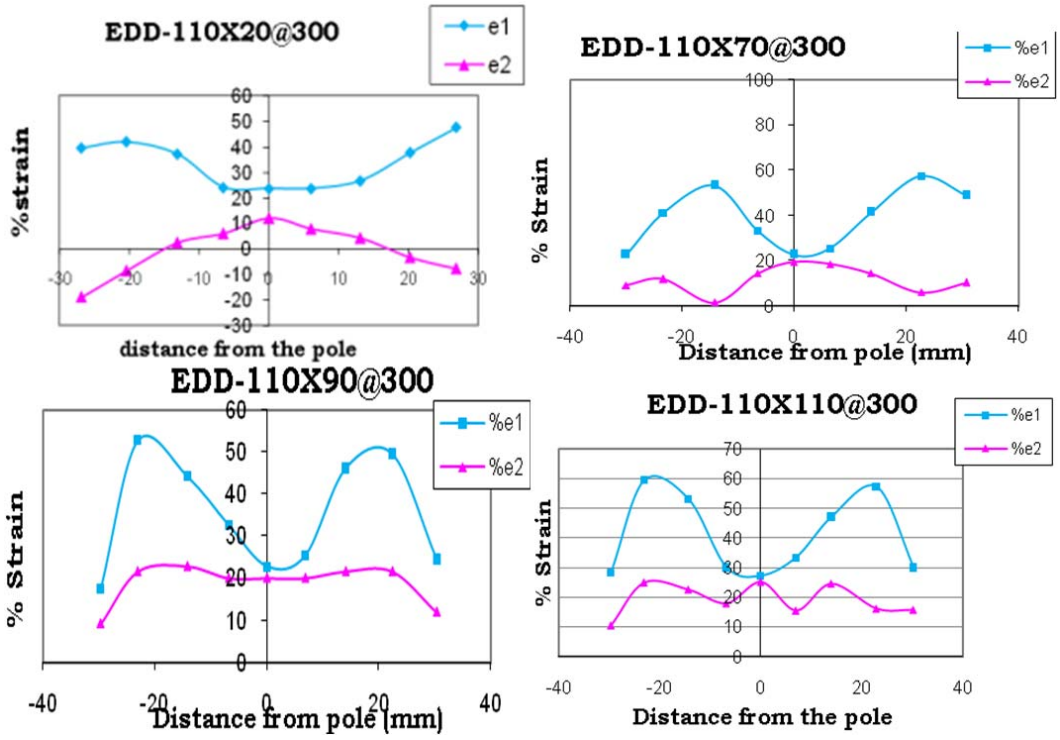

Fig. 7 Strain Distribution Profiles at 300^{0}C temperature

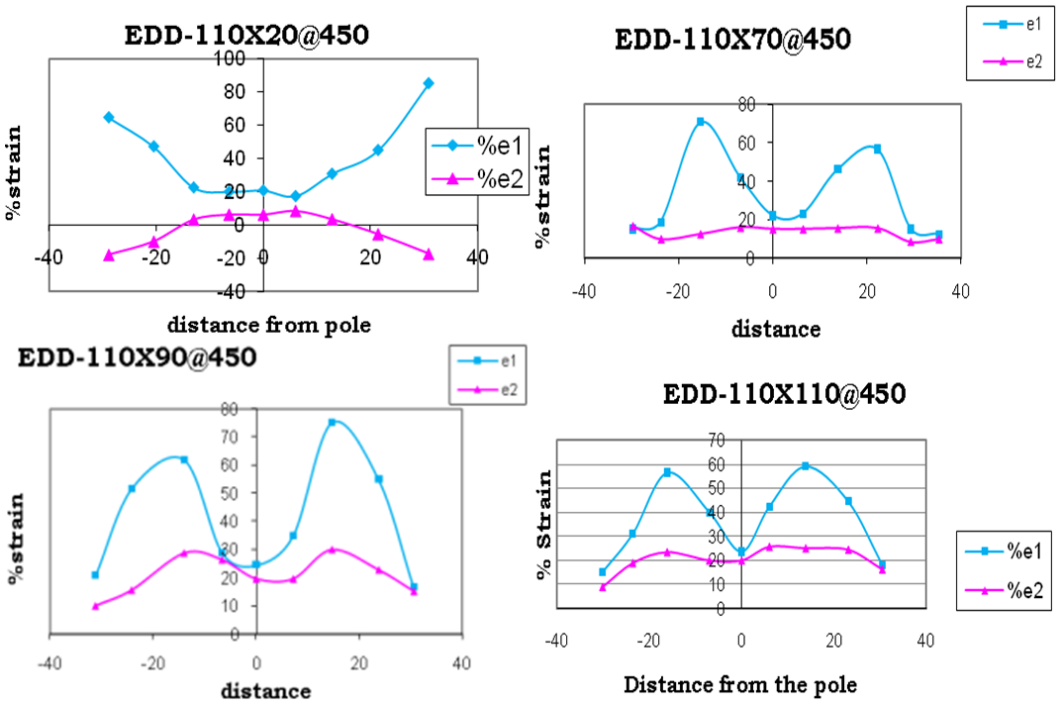

Fig. 8 Strain Distribution Profiles at 300^{0}C temperature

2. In case of minor strain, a similar trend was observed for blank widths 110mm, 100mm, 90mm, 80 mm which fall in biaxial stretching mode. For blank width 70mm, the minor strain is almost zero indicating plane strain condition. In this condition, the formability was observed to be minimum as indicated by lower peak strains and lower cup height at failure.
3. Below a blank width of 70 mm, the stretching component decreases in tangential direction (draw bead diameter being 72 mm) due to decreased gripping. So the minor strains progressively go down. When the blank width was decreased to 60 mm, minor strains became negative due to lateral drawing-in and with further decrease in blank width; the minor strains developed two peaks with negative values. This is due to change in stress state from biaxial tension to tension-compression (tension in the longitudinal and compression in the transverse directions).
4. As the blank width decreased, the separation between the two peaks increased progressively because of the increased lateral drawing-in of the sheet metal and correspondingly the failure site also moved away from the pole.

C. Metallurgical Studies

1. Grain Density

Figs. 9 and 10 represent the grain density of the stretched components at various temperatures and also for different sample sizes. It can be observed from Figs. 9 and 10 that for 110X50 mm specimen grain density is always lower as compared to 110X110 specimen (up to 300^{0}C). It is because when the width of specimen decreases due to drawing component compressive hoop stresses will appear in the region and as a result of that grain will be more elongated but the density will be slightly lower the elongated grains can be observed. From following images, it is also observed that there is not much change in the grain density of the component up to 300^{0}C.

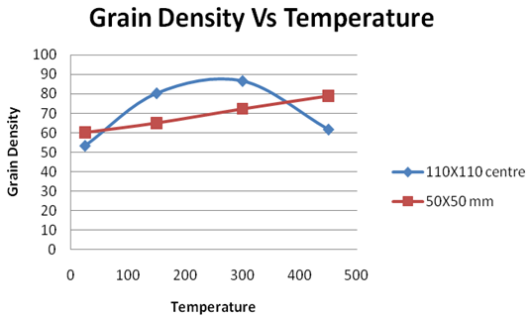

Fig. 9 Grain density graph at the centre of the specimen

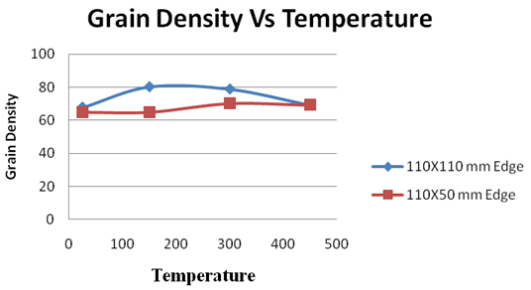

Fig. 10 Grain density graph at the Edge of the specimen

2. Microhardness

Fig. 11 represents microhardness in the fractured region of specimen at various temperatures. In this data, we can see that there is not much change in the microhardness value up to 300^0C it is because 300^0C is much below recrystallization temperature and microstructural changes are not accepted below this temperature. As investigated by [7] near 400^0C a phenomenon called Dynamic strain aging appears in the material primarily due to the presence of small amount of chromium when the load is applied there will be mobility of dislocations due to presence of Cr in a certain temperature band mobility of Cr becomes more than mobility of dislocations. So Cr breaks this dislocation into many parts due to this sudden increase in dislocation density material not only becomes slightly hard and brittle but also work hardening exponent of the material suddenly increases. This phenomenon can be seen in microhardness test that at 450^0C. There is almost 70% increase in the microhardness in the fracture region.

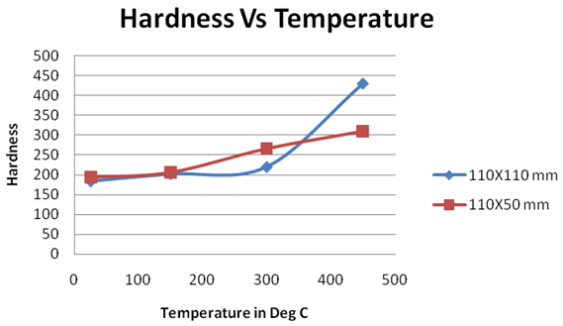

Fig. 11 Microhardness vs Temperature graph

IV. Conclusions

In order to understand the formability of EDD steel at elevated temperature the formability limit diagrams were constructed at different temperatures using Ni based super alloy dies. EDD steels are naturally formable at room temperature but their formability increases by increasing the temperature primarily because of decrease in the mean flow stresses .Specially at 450^oC the material exhibits higher formability due to the dynamic strain regime and same thing is experienced in the formability limit diagrams. It was seen from FLDs that for a substantial portion of sample plain strains were observed at all the temperatures.

Strain distribution profiles for EDD steel sheets were drawn at room temperature and at elevated temperatures to understand formability, strain path and fracture location of EDD steels completely at different temperatures.

Some microstructural studies were carried out on stretched specimens. It was observed that as the temperature increases the hardness increases and grain density increases up to 300^0C and decreases from 350^0C to 450^0C because of dynamic strain aging Phenomena.

References

[1] C. E. Dreyer, W. V. Chiu, R. H. Wagoner, A. R. Agnew, 2010. ‘‘Formability of a more randomly textured magnesium alloy sheet: Application of an improved warm sheet formability test.”, journal of materials Processing Technology, 210, 37-47 Graf. A, Hosford. w 1994, The influence of strain path changes on FLDs of alluminium 5111 T4, Int. j. mech. sci. 36, pp. 897-910.

[2] A. Graf, W. Hosford,“The influence of strain path changes on FLDs of alluminium” 5111 T4,Int.j.mech.sci.36,1994, pp. 897-910.

[3] A. K. Gosh, S. S. Hecker, Stretching limits in sheet materials in-plane verses out of plane deformation, metall. Trans A5A, 1974, pp. 16072-1616.

[4] S. S. Hecker, ‘‘Formability of aluminum alloy sheets”, journal of Engineering materials Technology, 1975, 97, pp. 66-73.

[5] D. Ravi Kumar, Formability analysis of extra-deep drawing steel, Journal of Material Processing Technology, 2002, 130, pp. 31-41.

[6] Stachowicz. F,. Effects of microstructure on the mechanical properties and limit strains in uniaxial and biaxial stretching, Journal of mach. work Technol.19, 1989, pp. 305-317

[7] Swadesh Kumar Singh, A K Gupta & K. Mahesh, CIRP J. Manf. Sci& Tech, 3, 2010, pp. 73–79.

[8] Swadesh kumar singh, K. Mahesh, Amith kumar Gupta, ‘‘Prediction of mechanical properties of extra deep drawn steel in blue brittle region using artificial neural network”, Journal of Materials and Design, 31, 2010, pp. 2288-2295.

[9] Sowerby. R, Duncan. J. L, Failure in sheet metal in biaxial tension Int. j. mech. Sci.13. 1971, pp. 217-229.

[10] Marciniak Z, Kuczynski K. Limit strains in the processes of stretch-forming sheet metal. International Journal of Mechanical Sciences, 9, 1967, pp. 609–20.

[11] Sachdev, A. K., Development of an Aluminium alloy sheet with improved formability, Metallurgical Transactions, 21A, 1990, pp. 165-175.

[12] Date, P. P. and K. A. Padmanabhan , On the formability of 3.15 mm thick low-carbon steel sheets, Journal of Materials Processing Technology, 35, 1992, pp. 165-180.

[13] Burford, D. A., K. Narasimhan and R. H. Wagoner, A theoretical sensitivity analysis of full-dome formability tests: Parametric study for n, m, r and, Metallurgical Transactions, 22A, 1991, pp. 1775-1778. Processing Technology, 35, 1992, pp. 165-180.

[14] Story, J. M., G. W. Jarvis, H. R. Zonker and S. J. Murtha, Issues and Trends in Automotive Aluminium sheet forming, Society of Automotive Engineers, 102, 1993, pp. 320-344.

[15] Hiam, J. and A. Lee , Factors influencing the forming limit curves of sheet steel, Sheet Metal Industries, 5, 1978, pp. 631-643.

[16] Swaminathan, K. and K. A. Padmanabhan, Some investigations on the forming behaviour of an indigenous extra-deep drawing low carbon steel-part-I: Experimental results, Trans. Indian Inst. Met., 44, 1991, pp. 231-247.

[17] Ravi Kumar, D. and K. Swaminathan, Formability of two Al alloys, Material Science and Technology, 15, 1999, pp. 1241-1252.

[18] Schedin, E. and A. Melander, On the strain distribution during the stretch forming on low and high strength sheet steels. Journal of Mechanical Working Technology, 15, 1987, pp. 181-202.

[19] Yang, T. S. and T. C. Hsu, Forming limit analysis of hemispherical punch stretch forming, Journal of Materials Processing Technology, 117, 2001, pp. 32-36.

[20] Fekete, J. R., Overview of sheet metal for stamping, Society of Automotive Engineers, 106, 1997, pp. 699-710.